

中国激光

高重复频率、窄脉冲声光调 Q 射频波导 CO₂ 激光器

吴名俊^{1,2}, 谭荣清^{1,2*}, 李辉¹, 宁方晋¹, 郑义军¹, 朱子任^{1,2}, 白进周^{1,2}

¹中国科学院空天信息创新研究院激光工程技术研究中心, 北京 100094;

²中国科学院大学电子电气与通信工程学院, 北京 100049

摘要 为实现高重复频率、窄脉冲激光输出, 研制了一台声光调 Q 射频波导 CO₂ 激光器。首先, 采用矩形波导耦合损耗理论分析了波导耦合效率与全反镜曲率半径、全反镜到波导口距离的关系, 获得了波导耦合损耗较小时的优化参数。其次, 研究了工作气压与激光输出的关系, 以及脉冲拖尾长度与 Q 开关开启时间的关系。当工作气压为 6.5 kPa, Q 开关开启时间为 0.6 μs 时, 获得了无拖尾脉冲波形, 并分析了峰值功率、平均功率、脉宽等参数随重复频率的变化规律。设计的激光器可实现重复频率 1 Hz~100 kHz 可调。当 Q 开关开启时间为 0.6 μs、重复频率为 1 kHz 时, 获得的脉冲宽度为 108.2 ns, 峰值功率为 2809.6 W; 当重复频率为 100 kHz 时, 脉宽为 135.1 ns, 峰值功率为 257 W。当重复频率为 70 kHz 时, 测得 x 和 y 方向上的光束质量因子分别为 1.50 和 1.21。

关键词 激光器; 波导 CO₂ 激光器; 高重复频率; 窄脉冲宽度; 声光调 Q

中图分类号 TN248.2

文献标志码 A

DOI: 10.3788/CJL230526

1 引言

高重复频率、窄脉冲 CO₂ 激光在非金属加工^[1]、激光医疗^[2-3]、极紫外(EUV)光刻机光源^[4-6]、光电对抗^[7-8]等领域中有广阔的应用前景。射频激励波导 CO₂ 激光器具有体积小、效率高、寿命长、免维护等优点, 连续波输出的 CO₂ 激光器已得到广泛应用^[9]。射频激励波导 CO₂ 激光器实现高峰值功率脉冲输出的主要技术手段有电光调 Q、机械调 Q、声光调 Q 等。电光调 Q 可以实现重复频率在 100 kHz 以上、脉宽为几十纳秒的脉冲激光输出, 但所需的 CdTe 等电光晶体生长困难、易损伤且价格昂贵, 晶体所需的驱动电压达数 kV 以上, 技术相对复杂^[10]; 机械调 Q 结构简单、成本较低, 但是受限于电机的转速和斩波器高速运转时的稳定性, 难以获得高重复频率的稳定脉冲输出, 且无法对脉冲进行精确时序控制及编码^[11]; 声光调 Q 则通常是将声光调制器置于谐振腔内, 通过声光衍射调节腔内损耗以实现调 Q 脉冲输出, 具有器件成本低、损伤阈值高等优点^[12]。

国内外对射频波导调 Q CO₂ 激光器的研究主要集中在电光调 Q 和机械调 Q。1979 年, Marcus 等^[13]报道了电光 Q 开关波导 CO₂ 激光器, 最高重复频率可达 345 kHz, 低重复频率下的脉冲宽度为 70 ns、峰值功率为 970 W。2006 年, Wang 等^[14]采用电光调 Q 方式, 在双通道波导 CO₂ 激光器中实现了最高

重复频率 70 kHz, 当重复频率为 10 kHz 时, 实现了脉冲宽度为 150 ns、峰值功率为 730 W 的脉冲输出。2013 年, Zhang 等^[15]在射频波导 CO₂ 腔内放置望远镜系统以聚焦光束, 运用机械斩波调 Q 技术获得了重复频率最高为 20 kHz 的脉冲输出, 此时获得的最高输出峰值功率为 730 W, 脉宽为 200 ns。2022 年, 潘其坤等^[16]在射频波导腔内放置斩波器进行机械调 Q, 在 1 kHz 时获得脉冲宽度为 350 ns、峰值功率最高为 3.7 kW 的脉冲输出。关于声光调 Q 射频波导 CO₂ 激光器, 国内外的报道较少。2019 年, Shrestha 等^[17]采用声光调 Q 技术和功率放大技术, 在射频波导 CO₂ 激光器中实现了重复频率达 200 kHz、峰值功率最高为 10.7 kW 的脉冲输出, 但脉冲宽度为 400 ns。

射频波导 CO₂ 激光器的腔镜与波导口之间的低损耗耦合条件较为严格^[18], 在波导管和腔镜之间插入声光 Q 开关元件后, 实现低耦合损耗更为困难。为了实现高重复频率、窄脉冲输出, 本文首先运用波导耦合损耗理论分析了全反镜到波导口的距离、全反镜曲率半径与耦合效率的关系, 确定了谐振腔参数。然后采用声光调 Q 方式, 优化工作气压和 Q 开关的开启时间, 使最高重复频率达到 100 kHz, 当重复频率为 1 kHz 时, 实现了峰值功率为 2809.6 W、脉宽为 108.2 ns 且无拖尾的脉冲激光输出。

收稿日期: 2023-02-14; 修回日期: 2023-03-20; 录用日期: 2023-04-05; 网络首发日期: 2023-04-15

基金项目: 国家自然科学基金(61775215)、中国科学院科研仪器设备研制项目(YJKYYQ20190041)

通信作者: *rongqingtan@163.com

2 实验设计及装置

2.1 波导耦合理论

对于波导激光器而言,波导端口与反射镜之间的耦合损耗是激光器谐振腔的一个至关重要的损耗,耦

合损耗由波导管和反射镜的参数共同决定。图 1 所示为波导耦合理论计算模型示意图,在波导中,场从 $A_0(x_0, y_0)$ 点出发,到达反射镜上 $A_1(x_1, y_1)$ 点后反射回波导口 $A_2(x_2, y_2)$ 点。由波导耦合损耗理论可知,矩形波导中 $A_0(x_0, y_0)$ 点的场分布^[19-21]可表示为

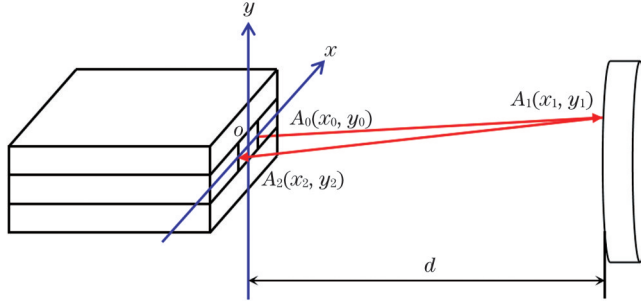


图 1 波导耦合计算模型

Fig. 1 Calculation model of waveguide coupling

$$E_{pq}(x_0, y_0) = \begin{cases} (ab)^{-\frac{1}{2}} \cos\left(\frac{p\pi x_0}{2a}\right) \cos\left(\frac{q\pi y_0}{2b}\right), & p \text{ and } q \text{ are odd numbers} \\ (ab)^{-\frac{1}{2}} \sin\left(\frac{p\pi x_0}{2a}\right) \sin\left(\frac{q\pi y_0}{2b}\right), & p \text{ and } q \text{ are even numbers} \end{cases}, \quad (1)$$

式中: a 和 b 分别为矩形波导截面的半宽度和半高度; y 方向节线数量为 $p-1$, x 方向节线数量为 $q-1$ 。由菲涅耳-基尔霍夫衍射理论可知, $A_0(x_0, y_0)$ 点处的场被反射镜反射回波导管端口后, $A_2(x_2, y_2)$ 处的场分布为

$$E_{p'q'}(x_2, y_2) = -\left[\frac{1}{\lambda^2 d^2 (ab)^{\frac{1}{2}}} \right] \exp(2jkd) \exp\left[\frac{jk(x_2^2 + y_2^2)}{2d}\right] \times \int_{-\infty}^{\infty} \exp\left(\frac{-j k x_1 x_2}{d}\right) \exp\left[\frac{j k x_1^2 (1 - d/R)}{d}\right] dx_1 \times \int_{-a}^a \exp\left(\frac{-j k x_0 x_1}{d}\right) \exp\left(\frac{j k x_0^2}{2d}\right) \cos\left(\frac{p\pi x_0}{2a}\right) dx_0 \times \int_{-\infty}^{\infty} \exp\left(\frac{-j k y_1 y_2}{d}\right) \exp\left[\frac{j k y_1^2 (1 - d/R)}{d}\right] dy_1 \times \int_{-b}^b \exp\left(\frac{-j k y_0 y_1}{d}\right) \exp\left(\frac{j k y_0^2}{2d}\right) \cos\left(\frac{q\pi y_0}{2b}\right) dy_0, \quad (2)$$

式中: p 和 q 为奇数; d 为波导口到反射镜的距离; λ 为激光波长;波矢大小 $k = \frac{2\pi}{\lambda}$; R 为全反镜曲率半径。

$$E_{p'q'}(x_2, y_2) = -\left[\frac{1}{\lambda^2 d^2 (ab)^{\frac{1}{2}}} \right] \exp(2jkd) \exp\left[\frac{jk(x_2^2 + y_2^2)}{2d}\right] \times \int_{-\infty}^{\infty} \exp\left(\frac{-j k x_1 x_2}{d}\right) \exp\left[\frac{j k x_1^2 (1 - d/R)}{d}\right] dx_1 \times \int_{-a}^a \exp\left(\frac{-j k x_0 x_1}{d}\right) \exp\left(\frac{j k x_0^2}{2d}\right) \sin\left(\frac{p\pi x_0}{2a}\right) dx_0 \times \int_{-\infty}^{\infty} \exp\left(\frac{-j k y_1 y_2}{d}\right) \exp\left[\frac{j k y_1^2 (1 - d/R)}{d}\right] dy_1 \times \int_{-b}^b \exp\left(\frac{-j k y_0 y_1}{d}\right) \exp\left(\frac{j k y_0^2}{2d}\right) \sin\left(\frac{q\pi y_0}{2b}\right) dy_0, \quad (3)$$

式中: p 和 q 为偶数。

将 A_2 点处的模投影到 A_0 点处的模上,得到展开系数为

$$\chi_{pq}^{p'q'} = \int_{-a}^a \int_{-b}^b E_{pq}(x_0, y_0) E_{p'q'}(x_2, y_2) dx_2 dy_2, \quad (4)$$

式中: E_{pq} 为 A_0 点处的光场分布; $E_{p'q'}$ 为 A_2 点处的光场分布。则耦合效率为

$$C_{pq}^{p'q'} = |\chi_{pq}^{p'q'}|^2. \quad (5)$$

因此耦合损耗为 $1 - |\chi_{pq}^{p'q'}|^2$ 。

在不同全反镜曲率半径下,一定距离范围内最低阶损耗模的耦合效率随全反镜到波导口的距离 d 的变化如图 2 所示,可以看出,随着距离的增加,耦合效率逐渐减小,因此全反镜应尽量靠近波导口以降低耦合损耗。但在放置 Q 开关后,为防止偏离的 1 级衍射光进入波导口形成谐振,Q 开关与波导口间应保持适当距离。达到衍射极值时的布拉格角为

$$\theta_{\text{Bragg}} = \frac{\lambda f}{2v}, \quad (6)$$

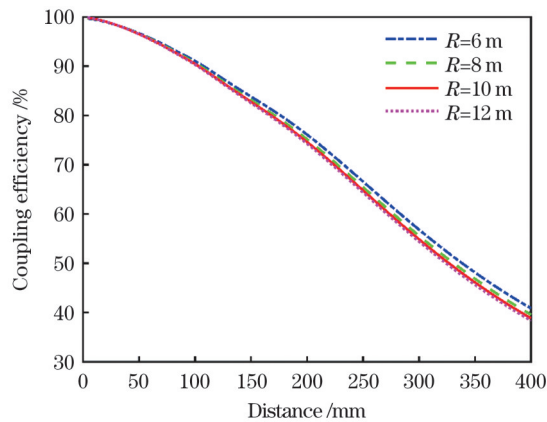


图 2 不同曲率半径下耦合效率与距离的关系

Fig. 2 Coupling efficiency versus distance under different curvature radii

式中: θ_{Bragg} 为布拉格角; f 为声光调制驱动器的射频信号中心频率; v 为超声波在单晶锗中的传播速度。取 $\lambda = 10.6 \mu\text{m}$, $f = 40 \text{ MHz}$, $v = 5.5 \text{ mm}/\mu\text{s}$, 由式(6)可得布拉格角为 2.2° , 因此, 在该布拉格角入射下 1 级衍射光偏离 0 级衍射光的角度为 4.4° 。本文采用的是截面尺寸为 $3 \text{ mm} \times 3 \text{ mm}$ 的方形波导, 为防止偏转的 1 级衍射光进入波导, 在波导口与 Q 开关之间应预留 40 mm 距离, 考虑 Q 开关放置空间, 波导口到全反镜的距离 $d = 60 \text{ mm}$ 。当 $d = 60 \text{ mm}$ 时, 耦合效率随全反镜曲率半径的变化如图 3 所示, 可以看出, 当曲率半径大于 2 m 时, 耦合效率可达 95% 以上, 且随着曲率半径的增加, 耦合效率趋于平稳。从图 2 可知, 当曲率半径 R 分别为 6 、 8 、 10 、 12 m 时, 耦合效率分别达 95.68% 、 95.55% 、 95.46% 、 95.39% , 且相差较小。我们选用曲率半径为 8 m 的凹面镀金玻璃全反镜开展实验。

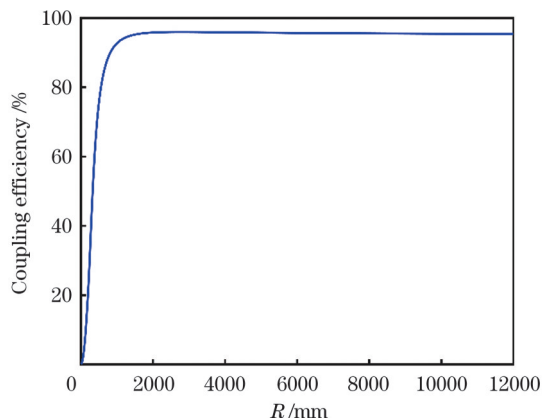
图 3 距离 $d=60 \text{ mm}$ 时耦合效率与曲率半径的关系

Fig. 3 Coupling efficiency versus curvature radius at distance $d=60 \text{ mm}$

2.2 实验装置

实验装置如图 4 所示, 波导通道为“Z”字形, 通道截面尺寸为 $3 \text{ mm} \times 3 \text{ mm}$, 上下电极为金属铝板, 折叠腔放电增益区总长度为 0.87 m , 谐振腔物理长度为

1.2 m , 激光器混合气体成分体积比为 $V_{\text{CO}_2}:V_{\text{N}_2}:V_{\text{He}}:V_{\text{xe}} = 19\%:19\%:5\%:5\%$, 总充气气压为 6.5 kPa 。光学谐振腔采用平凹腔, 全反镜 M_1 是曲率半径为 $R=8 \text{ m}$ 的凹面镀金镜片, 输出镜 M_4 为透过率 $T=30\%$ 的 ZnSe 镜片, M_2 和 M_3 为平面转折镜。密封窗口片为双面镀 $10.6 \mu\text{m}$ 增透膜的 ZnSe 平镜。声光调制器采用的声光晶体为单晶锗, 表面反射率 $<0.5\%$, 调制器偏振方向为水平偏振。射频驱动电源输出信号的中心频率为 40 MHz 。调制器有效通光孔尺寸为 $4 \text{ mm} \times 6 \text{ mm}$ 。

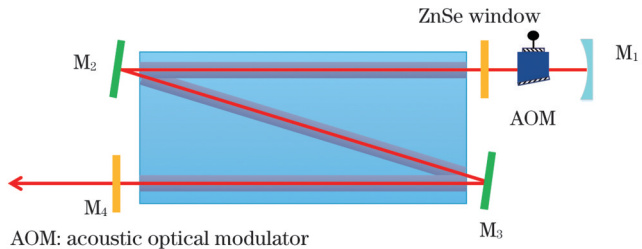


图 4 实验装置

Fig. 4 Experimental setup

3 分析与讨论

3.1 工作气压与激光输出的关系

对于气体激光器, 激光器内混合气体的工作气压对激光输出有着重要影响。因此, 在其他条件一定且 Q 开关开启时间为 $0.8 \mu\text{s}$ 的情况下, 研究了重复频率分别为 20 、 50 、 100 kHz 时峰值功率和脉宽随气压的变化规律。如图 5 所示, 当工作气压分别为 2.5 、 4.5 、 6.5 、 7.5 kPa 时, 峰值功率随气压的增加而逐渐增加, 在 6.5 kPa 时达到最大, 之后减小。这是由于电场强度 (E) 与气体粒子数密度 (N) 的比值 E/N 存在一个最佳范围, 在电场强度一定的条件下, 当气体压强过大即气体粒子数密度过大时, E/N 值偏离最佳范围, 从而导致能量有效转移至 CO_2 分子激发态的效率降低, 峰值功率减小。

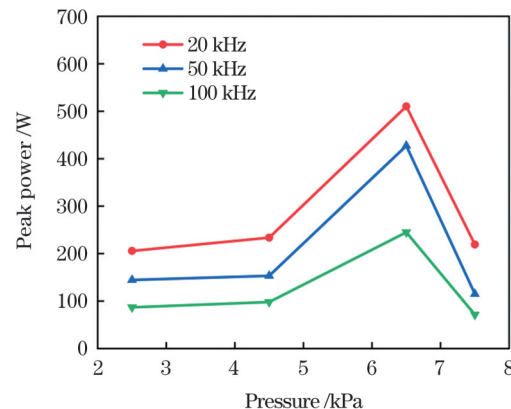


图 5 不同重复频率下峰值功率随气压的变化

Fig. 5 Peak power versus pressure under different repetition rates

图 6 所示为脉冲宽度随气压的变化,可以看出,当气压小于最佳气压 6.5 kPa 时,随着气压的增加,脉冲宽度略有减小,当气压高于 6.5 kPa 时,脉宽增大。这是由于随着气压的增加,CO₂ 激光上能级寿命缩短^[22],因此处于激发态的粒子能在较短的时间内跃迁至下能级,此时受激辐射产生的激光脉冲脉宽减小。而当气压进一步增加时,E/N 值偏离最佳范围,此时激光器放电稳定性变差,因此出现了功率减小以及脉宽增大的现象。

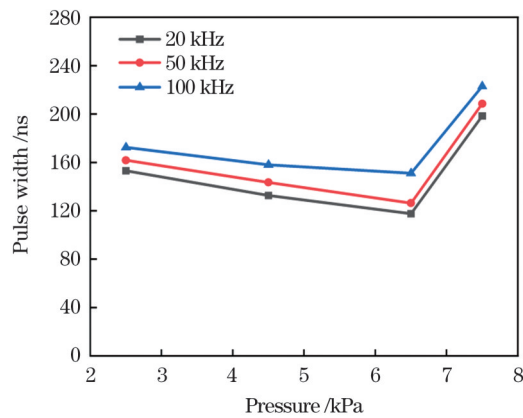


图 6 不同重复频率下脉冲宽度随气压的变化

Fig. 6 Pulse width versus pressure under different repetition rates

3.2 脉冲拖尾长度与 Q 开关开启时间的关系

当重复频率为 1 kHz,Q 开关的开启时间为 5 μs 时,测量得到的波形如图 7 所示,可以看出,脉冲波形存在一段较长的拖尾,拖尾的存在不利于峰值功率的提高,因此在一些实际应用场景中常常需要去除。

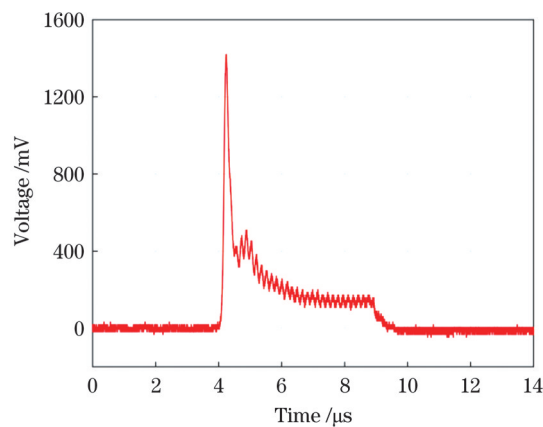


图 7 Q 开关开启时间为 5 μs 时的输出波形

Fig. 7 Output waveform when opening time of Q switch is 5 μs

为了探究影响拖尾长度的主要因素,当重复频率分别为 1、3、5、10、30 kHz,开启时间分别为 0.6、1.0、3.0、5.0、7.0 μs 时,测量拖尾长度随开启时间的变化,结果如图 8 所示,可以看出:拖尾长度随开启时间的缩

短而几乎呈线性减小,在 0.6 μs 时,脉冲拖尾完全消失;而当开启时间一定时,随着重复频率的增加,拖尾长度轻微减小。因此 Q 开关的开启时间是影响拖尾长度的主要因素,可以通过选取合适的开启时间来去除拖尾。

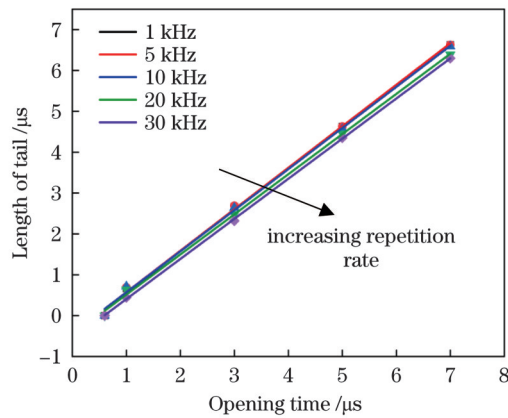


图 8 不同重复频率下拖尾长度与开启时间的关系

Fig. 8 Tail length versus opening time under different repetition rates

3.3 脉冲输出特性

对激光器工作气压以及 Q 开关开启时间等关键参数进行优化后,为获得较好的激光输出,选择工作气压为 6.5 kPa,Q 开关开启时间 $\tau=0.6 \mu\text{s}$,研究了脉冲输出波形、脉宽、峰值功率、平均功率、峰值功率放大系数等参数随重复频率变化的脉冲输出特性。重复频率为 1、20、50、100 kHz 时的输出波形如图 9(a)~(d) 所示,可以看到获得了接近高斯型的无拖尾波形。图 10 所示为脉冲宽度随重复频率变化的情况,随着重复频率的增加,脉宽略有增加,在重复频率为 1 kHz 时获得最窄脉宽 108.2 ns,在重复频率为 100 kHz 时,脉宽为 135.1 ns。

实验得到的平均功率和峰值功率随重复频率的变化如图 11 所示,随着重复频率的增加,平均功率逐渐增大,在重复频率增加到 70 kHz 以后,平均功率增长缓慢,当重复频率为 100 kHz 时,平均功率达到最大值 3.47 W。这是因为随着重复频率的增加,一个周期内反转粒子数积累的时间减少,但是输出脉冲个数增加,所以当重复频率不高时,随着重复频率的增加,平均功率增大。但是当重复频率增加到较大值时,一个周期内上能级反转粒子数积累的时间很短,虽然脉冲个数增加,但每个脉冲的能量减少,二者的共同作用导致高重复频率时平均功率的增加趋于平稳。峰值功率随着重复频率的增加逐渐减小,当重复频率为 1 kHz 时获得峰值功率 2809.6 W。当重复频率小于 10 kHz 时,随着重复频率的增大,峰值功率明显减小,当重复频率大于 10 kHz 时,峰值功率的减小逐渐变慢,高重复频率下趋于平稳。这是由于随着重复频率的增大,脉冲周期缩短,相应每周期内的储能时间减少,因此峰值功率

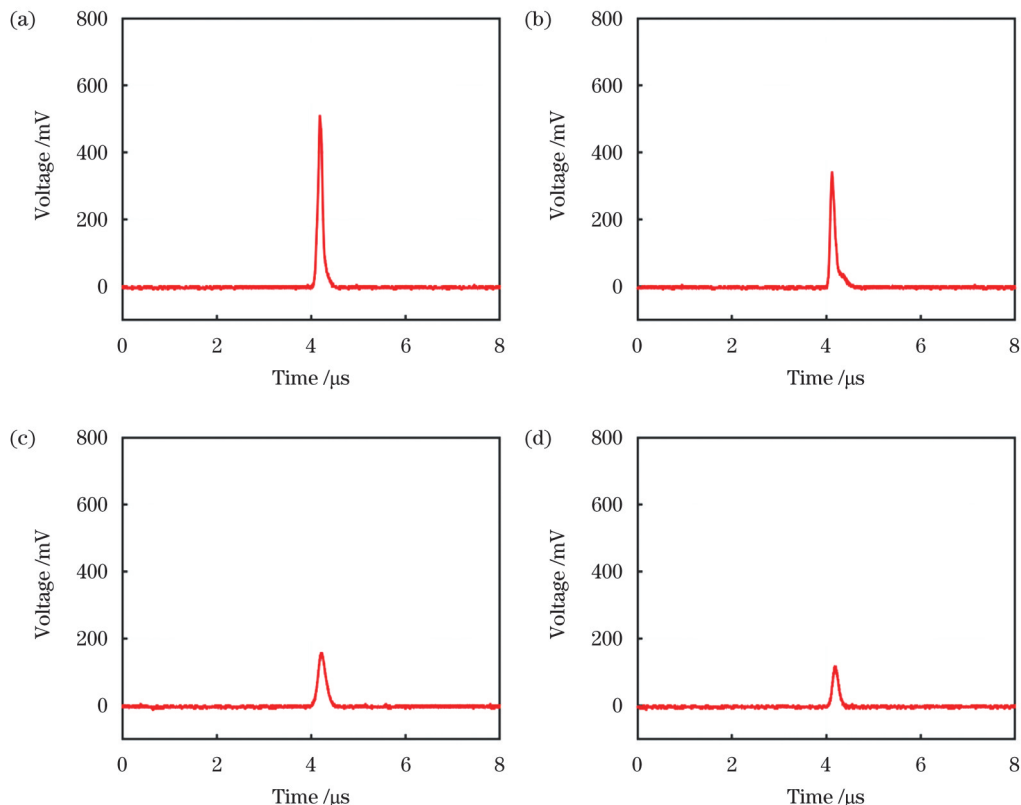


图 9 不同重复频率下的输出波形。(a) 1 kHz; (b) 20 kHz; (c) 50 kHz; (d) 100 kHz

Fig. 9 Waveforms under different repetition rates. (a) 1 kHz; (b) 20 kHz; (c) 50 kHz; (d) 100 kHz

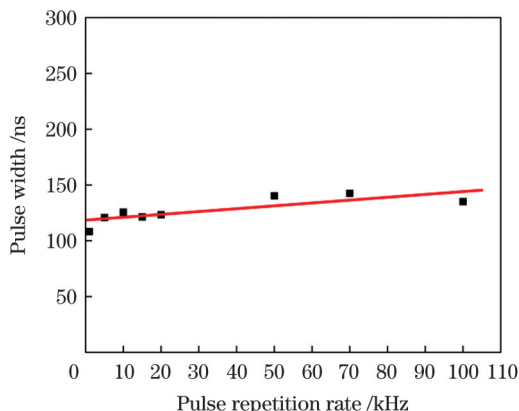


图 10 脉冲宽度随重复频率的变化

Fig. 10 Pulse width versus repetition rate

减小。

为了便于比较不同连续输出功率下激光器的调 Q 效果,采用峰值功率放大系数,即采用调 Q 时的峰值功率与不调 Q 时连续输出功率的比值作为衡量指标^[23]。在本实验中,激光器的连续输出功率为 9.1 W,在谐振腔内插入 Q 开关后连续输出功率下降为 8.2 W。当重复频率为 1 kHz 时,峰值功率为 2809.6 W,是不调 Q 时连续输出功率的 345 倍。当重复频率为 100 kHz 时,峰值功率为 257 W,是不调 Q 时

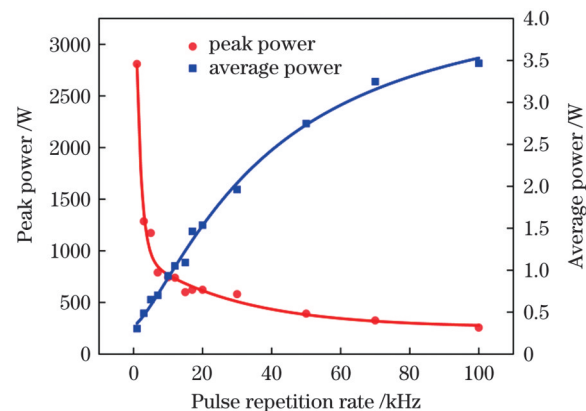


图 11 平均功率和峰值功率随重复频率的变化

Fig. 11 Average power and peak power versus repetition rate

连续输出功率的 31 倍。

3.4 光束质量

当 Q 开关开启时间为 0.6 μ s,工作气压为 6.5 kPa,重复频率为 70 kHz 时,实验采用焦距为 254 mm 的 ZnSe 聚焦透镜,通过刀口法测量得到的光束质量如图 12 所示,计算得到 x 和 y 方向的束腰直径分别为 $d_x = 0.76$ mm 和 $d_y = 0.74$ mm,全角发散角分别为 $\theta_x = 26.86$ mrad 和 $\theta_y = 21.99$ mrad,光束质量因子分别为 $M_x^2 = 1.50$ 和 $M_y^2 = 1.21$ 。

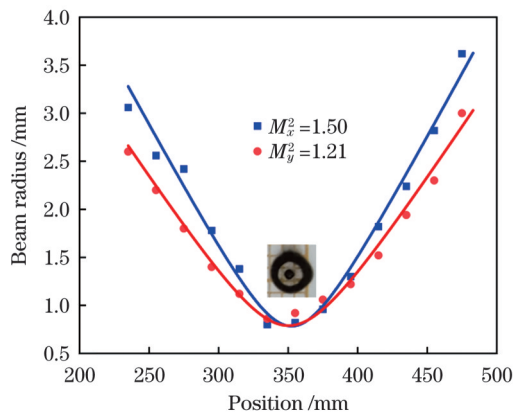


图 12 光束质量因子测量结果, 插图为光束强度分布图

Fig. 12 Measurement results of beam quality factors with distribution of beam intensity shown in inset

4 结 论

采用声光调 Q 的方法实现了小型射频波导 CO₂ 激光器高重复频率、窄脉冲激光输出。利用波导耦合损耗理论, 通过仿真分析确定了较优的谐振腔参数。分析了工作气压对激光输出的影响, 在设定条件下, 确定了最优的气压为 6.5 kPa。研究了影响脉冲拖尾的主要因素, 通过优化 Q 开关开启时间得到了高重复频率、窄脉冲宽度且无拖尾的激光脉冲。当 Q 开关开启时间为 0.6 μs, 重复频率为 1 kHz 时, 获得脉冲宽度为 108.2 ns、峰值功率为 2809.6 W 的激光输出, 调 Q 时的峰值功率为不调 Q 时的 345 倍。实验测量得到 x 和 y 方向的光束质量因子分别为 1.50 和 1.21, 获得了较好的光束质量。研究结果为后续采用大增益体积波导腔实现高峰值功率、高重复频率、窄脉冲宽度激光输出提供了参考。

参 考 文 献

- [1] Zhao L J, Cheng J, Chen M J, et al. Formation mechanism of a smooth, defect-free surface of fused silica optics using rapid CO₂ laser polishing[J]. International Journal of Extreme Manufacturing, 2019, 1(3): 035001.
- [2] Silva C V, Mantilla T F, Engel Y, et al. The effect of CO₂ 9.3 μm short-pulsed laser irradiation in enamel erosion reduction with and without fluoride applications-a randomized, controlled *in vitro* study[J]. Lasers in Medical Science, 2020, 35(5): 1213-1222.
- [3] Badreddine A H, Couitt S, Donovan J, et al. Demineralization inhibition by high-speed scanning of 9.3 μm CO₂ single laser pulses over enamel[J]. Lasers in Surgery and Medicine, 2021, 53(5): 703-712.
- [4] Endo A, Abe T, Hoshino H, et al. CO₂ laser-produced Sn plasma as the solution for high-volume manufacturing EUV lithography[J]. Proceedings of SPIE, 2007, 6703: 670309.
- [5] Komori H, Abe T, Sumitani A, et al. Laser-produced plasma source development for EUV lithography[C]//2009 IEEE International Conference on Plasma Science-Abstracts, June 1-5, 2009, San Diego, CA, USA. New York: IEEE Press, 2009.
- [6] 林楠, 杨文河, 陈韫懿, 等. 极紫外光刻光源的研究进展及发展趋势[J]. 激光与光电子学进展, 2022, 59(9): 0922002.
- [7] Lin N, Yang W H, Chen Y Y, et al. Research progress and development trend of extreme ultraviolet lithography source[J]. Laser & Optoelectronics Progress, 2022, 59(9): 0922002.
- [8] 陈健, 高慧斌. 高重频 CO₂ 激光干涉技术研究[J]. 中国光学, 2018, 11(6): 983-990.
- [9] Chen J, Gao H B. Research on the interference technology of high repetition frequency CO₂ laser[J]. Chinese Optics, 2018, 11(6): 983-990.
- [10] 王东, 王非, 白冰, 等. 10.6 μm 脉冲激光对多晶硅探测器干扰损伤实验[J]. 激光与红外, 2015, 45(9): 1084-1087.
- [11] Wang D, Wang F, Bai B, et al. Experiment study on the jamming and damage thresholds of polycrystalline silicon detector irradiated by 10.6 μm pulsed CO₂ laser[J]. Laser & Infrared, 2015, 45(9): 1084-1087.
- [12] 唐霞辉, 秦应雄, 彭浩, 等. 大功率射频板条 CO₂ 激光器[J]. 中国激光, 2022, 49(12): 1201005.
- [13] Tang X H, Qin Y X, Peng H, et al. High power RF slab CO₂ laser[J]. Chinese Journal of Lasers, 2022, 49(12): 1201005.
- [14] 田兆硕, 成向阳, 王骐. 电光调 Q CO₂ 激光器进展[J]. 激光技术, 2003, 27(3): 208-210, 213.
- [15] Tian Z S, Cheng X Y, Wang Q. Developments of electric-optically Q-switched CO₂ laser[J]. Laser Technology, 2003, 27(3): 208-210, 213.
- [16] Sakai T, Hamada N. Q-switched CO₂ laser using intense pulsed RF discharge and high-speed rotating chopper[J]. Proceedings of SPIE, 1995, 2502: 25-30.
- [17] 何洋, 陆君, 陈飞, 等. 声光调 Q CO₂ 激光器的实验研究[J]. 红外与激光工程, 2015, 44(8): 2280-2285.
- [18] He Y, Lu J, Chen F, et al. Experimental researches on acoustooptic Q-switched CO₂ laser[J]. Infrared and Laser Engineering, 2015, 44(8): 2280-2285.
- [19] Marcus S, Carter G M. Electrooptically Q-switched CO₂ waveguide laser[J]. Applied Optics, 1979, 18(16): 2824-2826.
- [20] Wang Q, Tian Z S, Zhu Q S. Study on tunable Q-switched/cavity-dumped partial Z-fold CO₂ waveguide laser with two channels and common electrodes[C]//2006 International Workshop on Laser and Fiber-Optical Networks Modeling, June 29-July 1, 2006, Kharkiv, Ukraine. New York: IEEE Press, 2006: 54-61.
- [21] Zhang Y C, Tian Z S, Sun Z H, et al. High pulse repetition frequency RF excited waveguide CO₂ laser with mechanical Q-switching[J]. Infrared Physics & Technology, 2013, 58: 12-14.
- [22] 潘其坤, 苗昉晨, 司红利, 等. 紧凑型波长自动调谐脉冲 CO₂ 激光器[J]. 中国光学, 2022, 15(5): 1007-1012.
- [23] Pan Q K, Miao F C, Si H L, et al. Compact wavelength auto-tuning pulsed CO₂ laser[J]. Chinese Optics, 2022, 15(5): 1007-1012.
- [24] Shrestha R, Tibolt A, Wheeler R, et al. High average power Q-switched CO₂ laser[J]. Proceedings of SPIE, 2019, 10911: 109110P.
- [25] Hill C A, Hall D R. Coupling loss theory of single-mode waveguide resonators[J]. Applied Optics, 1985, 24(9): 1283-1290.
- [26] Laakmann K D, Steier W H. Waveguides: characteristic modes of hollow rectangular dielectric waveguides[J]. Applied Optics, 1976, 15(5): 1334-1340.
- [27] 王新兵, 徐启阳, 谢明杰, 等. 平板波导谐振腔的耦合损失和模式特征[J]. 光学学报, 1995, 15(11): 1515-1519.
- [28] Wang X B, Xu Q Y, Xie M J, et al. Coupling losses and mode properties of planar waveguide resonators[J]. Acta Optica Sinica, 1995, 15(11): 1515-1519.
- [29] 李辉, 冯继东, 谭荣清, 等. 矩形波导 CO₂ 激光器谐振腔耦合效率研究[J]. 中国激光, 2017, 44(7): 0701003.
- [30] Li H, Feng J D, Tan R Q, et al. Coupling efficiency of CO₂ laser resonator with rectangular waveguide[J]. Chinese Journal of Lasers, 2017, 44(7): 0701003.
- [31] 楼祺洪. 脉冲放电气体激光器[M]. 北京: 科学出版社, 1993: 47-

48.

Lou Q H. Pulsed discharge gas laser[M]. Beijing: Science Press, 1993: 47-48.

[23] 蓝信矩. 激光技术[M]. 3 版. 北京: 科学出版社, 2009: 102-103.
Lan X J. Laser technology[M]. 3rd ed. Beijing: Science Press, 2009: 102-103.

Acousto-Optic Q-Switched Radio Frequency Waveguide CO₂ Laser with High Repetition Rate and Short Pulse Width

Wu Mingjun^{1,2}, Tan Rongqing^{1,2*}, Li Hui¹, Ning Fangjin¹, Zheng Yijun¹, Zhu Ziren^{1,2},
Bai Jinzhou^{1,2}

¹The Laser Engineering & Technology Research Center, Aerospace Information Research Institute, Chinese Academy of Sciences, Beijing 100094, China;

²School of Electronic, Electrical and Communication Engineering, University of Chinese Academy of Sciences, Beijing 100049, China

Abstract

Objective High-repetition-rate, short-pulse CO₂ lasers have broad application prospects in non-metal processing, laser medicine, extreme ultraviolet (EUV) lithography, photoelectric countermeasures, and other fields. Radiofrequency (RF)-excited waveguide CO₂ lasers are small, have high efficiency and long life, and are maintenance-free; thus, continuous-wave output CO₂ lasers have been widely used. The main technical means for RF-excited waveguide CO₂ lasers to achieve high peak power pulse outputs include electro-optical Q-switching, mechanical Q-switching, and acousto-optic Q-switching. Electro-optical Q-switching can achieve pulsed laser output with repetition rates of more than 100 kHz and pulse widths of tens of nanoseconds; however, electro-optical crystals, such as CdTe, are difficult to grow, easy to damage, and expensive, and the driving voltage required by the crystals is more than 1 kV; thus, the technology is relatively complex. The structure of mechanical Q-switching is simple and the cost is low; however, it is limited by the speed of the motor and the stability of the chopper at high speed. It is difficult to obtain a stable pulse output with a high repetition rate, and it is difficult to accurately control and encode the pulse. Acousto-optic Q-switching is normally realized by placing an acousto-optic modulator in the resonant cavity, and the loss in the cavity is modulated by acousto-optic diffraction to achieve a Q-switched pulse output, which has a low device cost and a high damage threshold. Acousto-optic Q-switched RF waveguide CO₂ lasers can achieve pulse output with high repetition rate and short pulse width. They have a compact structure and are easy to carry, thus providing high-quality laser sources for photoelectric countermeasures and other fields.

Methods The laser designed in this study adopts a semi-external cavity structure. An acousto-optic modulator is placed between the total reflection mirror and the window, and intracavity loss modulation is realized by the acousto-optic diffraction effect. Using rectangular waveguide coupling theory, the relationship between the coupling efficiency at the waveguide port and the curvature radius of the total reflection mirror, the distance from the total reflection mirror to the waveguide port, and the optimal total reflection mirror parameters are obtained. The position of the acousto-optic modulator in the cavity is determined using acousto-optic diffraction theory. Using an experimental method, the pulse output with high repetition rate and short pulse width is realized by optimizing the working pressure and opening time of the Q-switch. The beam quality is measured using the knife-edge method.

Results and Discussions The relationship between the waveguide coupling efficiency and the distance from the total reflection mirror to the waveguide port (Fig. 2) and the curvature radius of the total reflection mirror are determined (Fig. 3). It is found that a higher coupling efficiency can be obtained when the total reflection mirror is 60 mm away from the waveguide port with a curvature radius of 8 m. Through experiments, the relationship between the laser output and working pressure is determined. With an increase in the working pressure, the peak power first increases and then decreases (Fig. 5), and the pulse width decreases slightly and then increases (Fig. 6). The highest peak power and shortest pulse width are achieved at a working pressure of 6.5 kPa. This is because an appropriate increase in the working pressure shortens the lifetime of the upper energy level, and thus, the pulse width is compressed. However, when the working pressure is further increased, the ratio of electric field strength to gas particle number density (E/N) deviates from the optimal range, resulting in unstable discharge, a decrease in peak power, and an increase in pulse width. In addition, the results show that the pulse tail length decreases nearly linearly with a decrease in the opening time of the Q-switch (Fig. 8). Therefore, the tail can be effectively removed by optimizing the opening time of the Q-switch. A near-Gaussian tail-free waveform is obtained at the opening time of 0.6 μs. Finally, the influence of repetition rate on the output is determined when the working pressure is 6.5 kPa and the opening time is 0.6 μs. The pulse width increases slightly with an increase in the repetition rate (Fig. 10). The peak power gradually decreases, whereas the average power gradually increases with an increase in the repetition rate. Both tend to stabilize when the repetition rate is greater than 70 kHz (Fig. 11). The laser can achieve repetition rates of 1 Hz–100 kHz. A maximum peak power of 2809.6 W and pulse width of 108.2 ns are obtained at 1 kHz. At the repetition rate of 100 kHz, the pulse width is 135.1 ns and the peak power is 257 W. At the repetition rate of 70 kHz, the beam quality factors in the x and y

directions M_x^2 and M_y^2 are 1.51 and 1.20, respectively (Fig. 12).

Conclusions An RF waveguide CO₂ laser with a high repetition rate and short-pulse laser output is achieved using acousto-optic Q -switching. In this study, the waveguide coupling loss theory is used to determine the optimal resonant cavity parameters through simulation analysis. The effect of the working pressure on the laser output is analyzed, and the optimal pressure is determined to be 6.5 kPa under the experimental conditions. The main factor affecting the pulse tail, which is caused by the long Q -switch opening time, is determined or investigated. A tail-free pulse waveform with high repetition rate and short pulse width is obtained by optimizing the Q -switch opening time. A laser output with the pulse width of 108.2 ns and peak power of 2809.6 W is obtained at the Q -switch opening time of 0.6 μ s and repetition rate of 1 kHz. The peak power with Q -switch is 345 times that without Q -switch. The beam quality factors in the x and y directions M_x^2 and M_y^2 are 1.50 and 1.21, respectively, and the good beam quality is obtained. The study provides a reference for a subsequent realization of high peak power, high repetition rate, and short pulse-width laser output using a large-gain-volume waveguide cavity.

Key words lasers; waveguide CO₂ lasers; high repetition rate; short pulse width; acousto-optic Q -switching